Self-Organized Mixed Canonic-Dissipative Dynamics for Brownian Planar Agents

Guillaume Sartoretti and Max-Olivier Hongler
EPFL - STI/IMT/LPM
CH -1015 Lausanne (Switzerland).

July 29, 2014

Abstract

We consider a collection of N homogeneous interacting Brownian agents evolving on the plane. The time continuous individual dynamics is jointly driven by mixed canonical-dissipative (MCD) type dynamics and White Gaussian noise sources. Each agent is permanently at the center of a finite size observation disk D_ρ. Steadily with time, agents count the number of their fellows located in D_ρ. This information is then used to re-actualize control parameters entering into the MCD. Dissipation mechanisms together with the noise sources ultimately drive the dynamics towards a consensus stationary regime characterized by an invariant measure P_s on an appropriate probability space. Assuming propagation of chaos, a mean field approach enables to analytically calculate P_s. For each agent, our dynamics naturally implements: i) a tendency to not be isolated, ii) a tendency to avoid strong promiscuity, and iii) an overall tendency to be attracted to a polar point. The MCD drift is derived from an Hamiltonian function $\mathcal{H}$ and it incites the agents to follow one consensual orbit which coincides with a level curve of $\mathcal{H}$. When $\mathcal{H}$ is the harmonic oscillator Hamiltonian, we are able to analytically derive the corresponding consensual circular orbit as a function of the size of the observation disk V_ρ. Generalizations involving more complex $\mathcal{H}$ are explicitly worked out. Among these illustrations, we study an Hamiltonian for which the level curves are the Cassini's ovals. This enables to generate consensus trajectories exhibiting different topologies which only depend on the observation range of the agents. A selection of simulations experiments corroborating the theoretical findings are presented.

Keywords: homogeneous Brownian agents - limited-range mutual interactions - consensus orbit generation - mixed canonical-dissipative dynamics - mean-field description - analytical results.

1 Introduction

The emergence of structured collective dynamical patterns from simple agent level behaviors as observed in nature for fishes, birds, insects and the like inspires a sustained research activity in management and control of complex systems, and particularly in the domain of swarm robotics. The capability of agents to act asynchronously to determine specific trajectories by relying only on local sensing is definitely attractive when a centralized control becomes unfeasible - for example to coordinate large assemblies of autonomous robots or other agents. One possibility to address these global control difficult issues, is to try to implement dynamic strategies where identical robots are programmed with elementary features requiring limited on-board real time sensing and computational resources. This general and truly simple idea triggers a strong interdisciplinary research activity which, as emphasized in the recent review [3], encompasses a relatively wide spectrum of perspectives ranging from ethology to swarm robotics. Focusing here on the dynamic system and control perspectives, we study a collection of asynchronously interacting point Brownian agents obeying elementary coordination algorithms. The basic ingredients of our modeling are: i) an Hamiltonian function $\mathcal{H}$ which provides a parametric family of non-intersecting level curves defining closed orbits, ii) a mixed conservative and gradient vector field constructed from $\mathcal{H}$ involving one (or several) control parameters, iii) a stochastic driving stylized by WGN's sources and iv) for each agent, a circular observation range V_ρ with radius ρ, centered at each agent location. Agents mutual interactions directly depend on the size of V_ρ. Interactions produce an adaptive mechanism which drive the agents to ultimately adopt one (or several) consensus value(s) of the control parameter(s). The emerging consensus parameter(s) value selects one specific orbits among the Hamiltonian parametric family. For such mixed canonic-dissipative stochastic dynamics, connected with models discussed in [6], we are able to explicitly write the resulting invariant probability measure solving the associated time-independent NLFP. We therefore can investigate analytically the influence of the radius ρ of observation range V_ρ on the emerging consensus dynamic achieved by the agents. While our class of dynamics presents similarities with potential-ruled algorithms as those used for example in [4, 3, 7, 11], it however keeps a decentralized mechanism stylized in the basic agents models pioneered by [9, 12] and more recently by [1].

Mathematically speaking, our modeling relies on a set of N continuous time, coupled nonlinear stochastic differential equation (SDE) driven by White Gaussian noise (WGN). In this context, the basic formal question, first raised first by H. McKean [8], is to calculate the limit of the probability distribution which describes a large agent collection (i.e. formally the thermodynamic limit $N \to \infty$) and then fluctuations around this limit for finite N. Considering that all agent have identical independent initial conditions, one mathematically expect (this can be rigorously proved under somehow restricting technical hypothesis) that in the thermodynamic limit, all finite number of agents behaves independently of the other ones and they all can be described by the same probability distribution (this is known as *propagation of chaos*). The common probability distribution solves a Markovian evolution described by a nonlinear Chapman-Kolmogorov type partial differential equation. Accordingly, when propagation of chaos holds, we may characterize the dynamic behavior of the global population by only studying the dynamics of a single, randomly chosen, agent subject to an effective external *mean-field* generated by its surrounding fellows. In presence of WGN's sources, the single representative agent is a diffusion process and its probability measure obeys to a non-linear *Fokker-Planck* equation (NLFP), [2].

2 Interacting Brownian agents driven by canonic-dissipative dynamics and White Gaussian Noise

We consider a swarm of N mutually interacting dynamical agents a_k for $k = 1, 2, \cdots, N$ evolving on the plane $\mathbb{R}^2$ with state variables $\vec{X}(t) = (X_1(t), X_2(t), \cdots, X_N(t))$. In this section, we assume the homogeneous situation in which all individual isolated agents a_k are dynamically identical. The collective dynamics is assumed to obey an N-dimensional diffusion process on $\mathbb{R}^2$ given by a set of stochastic differential equations (SDE):

$$\begin{cases} d\mathbf{X}_k(t) = \mathbb{A}_k(t) \cdot \mathbf{X}_k(t)\, dt + \underbrace{\gamma \left[\mathcal{L}^2_{k,\rho}(t) - \|\mathbf{X}_k(t)\|^2_2\right] \mathbf{X}_k(t)}_{\mathcal{C}_k(\mathbf{X}_k(t))}\, dt + \sigma\, d\mathbf{W}_k(t), \qquad k = 1, 2, \cdots, N, \\ \\ \mathbf{X}_k(0) = \mathbf{X}_{0,k}, \qquad \text{and} \qquad \mathbf{X}_k(t) \in \mathbb{R}^2. \end{cases} \tag{1}$$

In Eq.(1), the following notations are used: $\mathbf{X}_k(t) = (x_{k,1}(t), x_{k,2}(t)) \in \mathbb{R}^2$, the usual norm $\|\mathbf{X}_k(t)\|^2_2 := \left(x^2_{k,1}(t) + x^2_{k,2}(t)\right)$, γ and σ are positive constants common to all a_k (i.e. homogeneity assumption) and $\mathbf{W}_k(t) = (W_{k,1}, W_{k,2})$ are independent standard Brownian Motions (BM) and hence the formal differentials $dW_k(t)$ are White Gaussian Noise (WGN) processes. The agents interactions will be defined via the scalars $\mathcal{L}^2_{k,\rho}(t)$ and the matrices $\mathbb{A}_k(t)$ which both will depend on $V_{k,\rho}(t)$ the set of instantaneous neighboring fellows surrounding agent a_k at time t. For a given observation range ρ, the a_k-*instantaneous observation neighborhood* $\mathcal{D}_{k,\rho}(t)$ is the disk:

$$\mathcal{D}_{k,\rho}(t) = \left\{\mathbf{X} \in \mathbb{R}^2 \mid \|\mathbf{X} - \mathbf{X}_k(t)\|_2 \leq \rho\right\} \tag{2}$$

and we define the indices set

$$V_{k,\rho}(t) = \{ i \mid \mathbf{X}_i(t) \in \mathcal{D}_{k,\rho}(t) \} . \tag{3}$$

which identifies the a_k-neighboring agents present in the disk $\mathcal{D}_{k,\rho}(t)$. We shall write $N_{k,\rho}(t) := |V_{k,\rho}(t)|$ the cardinality of the set $V_{k,\rho}(t)$. The dynamic elements contained in Eq.(2) and Eq.(3) are now used to characterize the agents' mutual interactions via a couple of contributions:

i) **Canonic-dissipative matrix** $\mathbb{A}_k(t)$. The dynamic matrix $\mathbb{A}_k(t)$ associated with agent a_k can now be defined as:

$$\mathbb{A}_k(t) := \begin{pmatrix} \frac{N_{k,\rho}(t)}{N} - \frac{1}{M} & \frac{N_{k,\rho}(t)}{N} \\ \\ -\frac{N_{k,\rho}(t)}{N} & \frac{N_{k,\rho}(t)}{N} - \frac{1}{M} \end{pmatrix}, \tag{4}$$

with $1 \leq M \leq N$ and $N_{k,\rho}(t)/N$ is the fraction of the total swarm that agent a_k detects in $\mathcal{D}_{k,\rho}(t)$ (we shall adopt the convention that agent a_k systematically detects itself implying that $V_{k,\rho}(t) \geq 1, \forall t$). As $\mathbf{X}_k = 0$ is a singular point of the deterministic dynamics (i.e. obtained for $\sigma = 0$ in Eq.(1)) the matrix $\mathbb{A}_k(t)$ formally stands for the linear mapping of the dynamics in the vicinity of the origin. The associated couple of eigenvalues of $\mathbb{A}_k(t)$ read:

$$\lambda_{k,\pm}(t) = \underbrace{\left[\frac{N_{k,\rho}(t)}{N} - \frac{1}{M} \right]}_{:=\mathcal{R}_k} \pm (\sqrt{-1}) \underbrace{\left[\frac{N_{k,\rho}(t)}{N} \right]}_{:=\mathcal{I}_k} := \mathcal{R}_k + i\,\mathcal{I}_k. \tag{5}$$

Hence, at a given time t, the real part in Eq.(5) expresses the non-conservative character of the dynamics (i.e. the divergence part of the VF). The singular point $\mathbf{0} \in \mathbb{R}^2$ is an attractive (respectively repulsive) node when $\mathcal{R}_k < 0$ (resp. $\mathcal{R}_k > 0$). In parallel, the component $\mathcal{I}_k$ expresses the rotational nature of the VF. In particular when $\mathcal{R}_k = 0$, the dynamics is conservative; it expresses the *Hamiltonian* component of the a_k-VF.

ii) **Adaptive limit cycle radius**. The scalar quantity

$$\mathcal{L}^2_{k,\rho}(t) := \frac{1}{|V_{k,\rho}(t)|} \sum_{j \in V_{k,\rho}(t)} \|X_j(t)\|_2^2 \tag{6}$$

defines the (square) of the radial position of the set-barycenter formed by agents belonging to $V_{k,\rho}$.

By construction, the generalized force $\mathcal{C}_k(X_k(t))$ in Eq.(1) drives any agent a_k towards a circle of radius $\mathcal{L}_{k,\rho}(t)$ and the component $\mathcal{I}_k(t)$ in Eq.(5) sets agents into circulation on this circle. The noise sources $dW_k(t)$ in the dissipative dynamics Eq.(1), progressively with time erase information regarding the initial configuration. The Fokker-Planck equation associated with the multi-variate diffusion process Eq.(1) evolving in $\mathbb{R}^{2N}$ reads:

$$\begin{cases} \partial_t P(\vec{\mathbf{x}}, t|\vec{\mathbf{x}}_0) = -\bigtriangledown \left\{ \left[\mathbb{A}_k(t) \cdot \mathbf{x}_k(t) + \gamma \left[\mathcal{L}^2_{k,\rho}(t) - \|\mathbf{x}_k(t)\|_2^2 \right] \mathbf{x}_k(t) \right] P(\vec{\mathbf{x}}, t|\vec{\mathbf{x}}_0) \right\} + \frac{\sigma^2}{2} \triangle P(\vec{\mathbf{x}}, t|\vec{\mathbf{x}}_0), \\ \\ P(\vec{\mathbf{x}}, t|\vec{\mathbf{x}}_0) : \mathbb{R}^{2N} \to \mathbb{R}^+, \quad \vec{\mathbf{x}} := (\mathbf{x}_1, \mathbf{x}_2, \cdots, \mathbf{x}_N), \quad \mathbf{x}_k := (x_{k,1}, x_{k,2}), \qquad k = 1, 2, \cdots, N. \end{cases} \tag{7}$$

Note that Eq.(7) is so far merely formal. Indeed, due to the agents' interactions, both $\mathbb{A}_k(t)$ and $\mathcal{L}^2_{k,\rho}(t)$ depend themselves on $P(\vec{\mathbf{x}}, t|\vec{\mathbf{x}}_0)$. Let us now assume that for N large, we can approximately adopt the mean-field (MF) view point. The MF approach assumes that the dynamic behavior of a single and randomly chosen agent a_k will provide a representative picture on the global dynamic. For identically and independently distributed initial conditions, the MF approach enables to write:

$$P(\vec{\mathbf{x}}, t|\vec{\mathbf{x}}_0) = [P(\mathbf{x}, t|\mathbf{x}_0)]^N := [P(\mathbf{x}, t|0)]^N \qquad \mathbf{x} = (x_1, x_2), \tag{8}$$

a property often referred in the literature as propagation of chaos. When the MF approach holds, one can state:

Proposition 1. *Consider the* **mixed-canonical dissipative diffusive dynamics** *Eq.*(1). *Asymptotically with times, the dynamics can be factorized as in Eq.*(8) *and the MF representative agent obeys to the couple of diffusion equations :*

$$\begin{cases} dX_1(t) = +\frac{1}{M} X_2(t) + \gamma \left[\mathcal{L}_{s,\rho}^2 - (X_1^2(t) + X_2^2(t))\right] X_1(t)\, dt + \sigma dW_1(t), \\ dX_2(t) = -\frac{1}{M} X_1(t) + \gamma \left[\mathcal{L}_{s,\rho}^2 - (X_1^2(t) + X_2^2(t))\right] X_2(t)\, dt + \sigma dW_2(t). \end{cases} \tag{9}$$

For weak noise (i.e. large values of γ/σ^2), the radius approximately reads $\mathcal{L}_{s,\rho} \simeq \frac{\rho}{\sqrt{2(1-\cos(\pi/M))}}$ and the associated stationary probability density $P_s(\mathbf{x})$ reads:

$$P_s(\mathbf{x}) dx_1 dx_2 = \mathcal{Z}^{-1} \exp\left\{\frac{2\gamma}{\sigma^2}\left[\mathcal{L}_{s,\rho}^2 - (x_1^2 + x_2^2)\right]\right\} dx_1 dx_2, \qquad \mathbf{x} = (x_1, x_2) \in \mathbb{R}^2, \tag{10}$$

with $\mathcal{Z}$ being the probability normalization factor.

Guidelines to prove Proposition 1.

The MF assumption and Eq.(8) lead us to focus on a single representative planar agent $\mathbf{X}(t) = (x_1(t), x_2(t))$, and we write:

$$\begin{cases} \partial_t P(\mathbf{x}, t|0) = -\nabla\left\{\left[\mathbb{A}(t)\,\mathbf{x} + \gamma\left[\mathcal{L}_\rho^2(t) - \|\mathbf{x}(t)\|_2^2\right]\mathbf{x}\right] P(\mathbf{x}, t|0)\right\} + \frac{\sigma^2}{2} \triangle P(\mathbf{x}, t|0), \\ P(\mathbf{x}, t|0) : \mathbb{R}^2 \to \mathbb{R}^+, \end{cases} \tag{11}$$

where we have dropped the (agent's identity) k-index, that is to say we wrote:

$$\frac{N_{k,\rho}(t)}{N} \mapsto \frac{N_\rho(t)}{N} = \int_{(\mathbf{x}) \in D_\rho} P(\mathbf{x}, t|0)\, dx_1\, dx_2 \tag{12}$$

and similarly:

$$\mathcal{L}_{k,\rho}^2(t) \mapsto \mathcal{L}_\rho^2(t) = \int_{(x_1,x_2) \in D_\rho} \left(x_1^2 + x_2^2\right) P(\mathbf{x}, t|0)\, dx_1\, dx_2 \tag{13}$$

and D_ρ is the representative agent's neighborhood. Asymptotically with time, the stochastic dissipative dynamics reaches a stationary regime will, due to symmetry, will be characterized by rotationally invariant probability measure. In this stationary regime, a time-independent probability current circulates with the angular velocity M^{-1} around the origin. The invariant probability density solves the stationary Fokker-Planck equation:

$$0 = -\nabla\left\{\left[\mathbb{A}_s\,\mathbf{x} + \gamma\left[\mathcal{L}_{s,\rho}^2 - \|\mathbf{x}\|_2^2\right]\mathbf{x}\right] P_s(\mathbf{x})\right\} + \frac{\sigma^2}{2} \triangle P_s(\mathbf{x}), \tag{14}$$

where the MF approach implies:

$$\lim_{N\to\infty}\left\{\lim_{t\to\infty} \frac{N_\rho(t)}{N}\right\} = \frac{N_{s,\rho}}{N} = M^{-1} \qquad \text{and} \qquad \lim_{t\to\infty} \mathcal{L}_\rho^2(t) = \mathcal{L}_{s,\rho}^2, \tag{15}$$

and therefore,

$$\lim_{t\to\infty} \mathbb{A}(t) = \mathbb{A}_s = \begin{pmatrix} 0 & M^{-1} \\ -M^{-1} & 0 \end{pmatrix}. \tag{16}$$

From a uniformly rotating coordinates' frame with angular velocity M^{-1}, the stationary regime dynamics becomes purely gradient and the resulting stationary probability density $P_s(\mathbf{x})$ solving Eq.(14) enjoys microscopic reversibility (i.e. *detailed balance*). It explicitly reads, [6]:

$$P_s(\mathbf{x})dx_1dx_2 = P_s(r)dr\,d\theta = \mathcal{N}(\mathcal{L}_{s,\rho})\, e^{\left[-\frac{\gamma}{\sigma^2}(r^2-\mathcal{L}^2_{s,\rho})^2\right]}d(r^2)\,d\theta. \tag{17}$$

with $\mathcal{N}^{-1}(\mathcal{L}_{s,\rho}) = \sqrt{\pi^3\sigma^2/\gamma}\,\mathrm{Erfc}\left(-\frac{\sqrt{\gamma}\,(\mathcal{L}^2_{s,\rho})}{\sigma})\right)$ being the normalization factor.

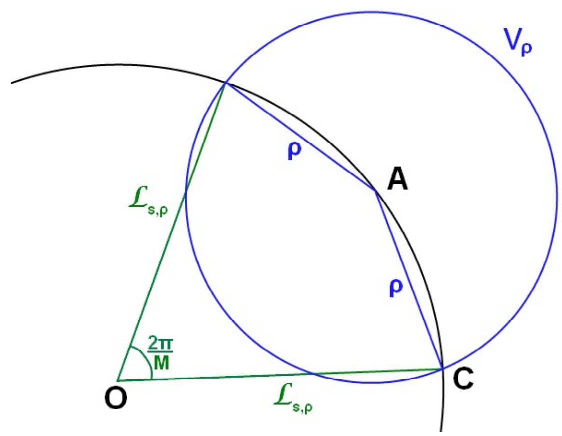

Figure 1: The cylindrical symmetry characterizing the stationary regime implies that the agents probability distribution is rotationally invariant with respect to **O**. Accordingly, there will be on average N/M agents located in a sector with an opening angle $2\pi/M$. For large γ/σ^2, these agents will be confined in the direct proximity of the circle of radius $\mathcal{L}_{s,\rho}$. Consider an arbitrary agent located at **A** with a stationary observation range $V_{s,\rho}$ with radius $\rho = \mathbf{AC}$. The set $V_{s,\rho}$ exactly encompasses the circular arc with aperture $2\pi/M$ thus ensuring that the agent at **A** has M/N neighboring fellows. The cosine theorem in the triangle **OAC** implies that $\mathcal{L}^2_{s,\rho} = 2\rho^2/\left[1-\cos(\pi/M)\right]$.

In this stationary regime, the stationary observation neighborhood $V_{s,\rho} := \lim_{t\to\infty} V_\rho(t)$ exactly encompasses a circular sector with aperture $\varphi(M)$ and radius $\mathcal{L}^2_{s,\rho}(M)$. Both $\varphi(M)$ and $\mathcal{L}_{s,\rho}(M)$ are adjusted to ensure that N/M agents are located in $V_{s,\rho}$. For large ratio $\frac{\gamma}{\sigma^2}$ (i.e. essentially a large signal-to-noise ratio), Eq.(17) exhibits a sharply peaked "Mexican hat" shape with its maximum on the circle $r = \mathcal{L}_{s,\rho}$ (i.e. almost all agents stay confined in the direct neighborhood of the circle $r = \mathcal{L}_{s,\rho}$). As detailed in Figure 1's caption, an elementary trigonometric argument enables to derive the compact relation:

$$\mathcal{L}_{s,\rho} = \frac{\rho}{\sqrt{2-2\cos(\pi/M)}}. \tag{18}$$

□

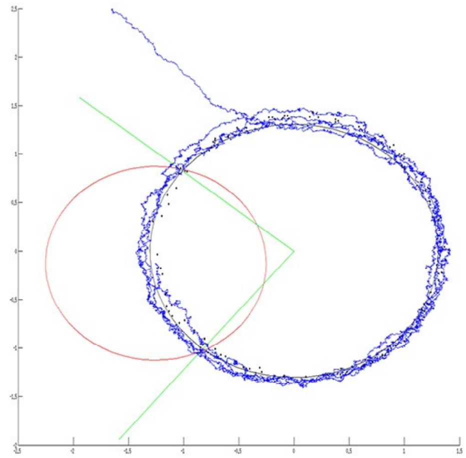

Figure 2: For a collection of $N = 100$ agents with $M = 4$ and $\rho = 1$. The observation range V_ρ encompasses exactly the sector of aperture $\pi/4$ to determine the size of the self-generated limit cycle (see the construction given in Figure 1). We explicitly draw the trajectory of a randomly chosen agent and observe that this agent indeed follows the consensual limit cycling orbit with analytically predicted radius $\mathcal{L}_{s,\rho} = \sqrt{2}\rho = \sqrt{2}$.

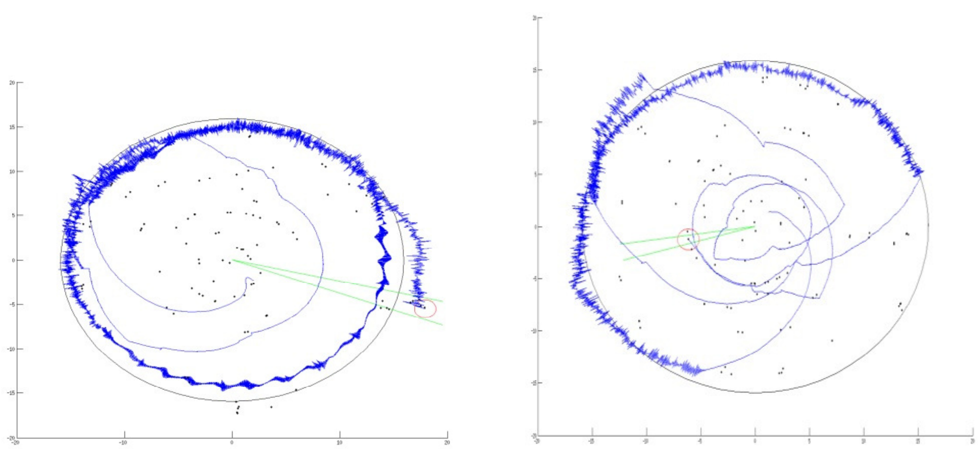

Figure 3: Left: For a collection of $N = 100$ agents with $M = 50$ and $\rho = 1$. The observation range V_ρ encompasses exactly the narrow sector of aperture $\pi/50$ to determine the size of the self-generated limit cycle (see the construction given in Figure 1). We explicitly draw the trajectory of a randomly chosen agent and observe that this agent indeed follows the consensual limit cycling orbit with analytically predicted radius $\mathcal{L}^2_{s,\rho} = 2/\left[1 - \cos(\pi/50)\right] \simeq (50/\pi)^2 \simeq (17)^2$.
Right: Another orbit realization for conditions fully similar.

Additional remarks. Observe that besides γ and σ which define an overall time scale, there are two additional control parameters in the dynamics Eq.(1):

a) **Hamiltonian parameter** M. The sector angle M into the canonic-dissipative matrix $\mathbb{A}(t)$. This parameter fixes the angular velocity $\omega = M^{-1}$ of the swarm and adjusts the size of the consensus limit cycle radius $\mathcal{L}_{s,\rho}$. For a given size of the observation disk with radius ρ and for large M, we have $\mathcal{L}_{s,\rho} \simeq \rho M/\pi$ and the angular velocity tends to vanish.

b) **Interaction range parameter** ρ. The radius of the observation disk ρ which directly determines the consensus size of the limit cycle radius $\mathcal{L}_{s,\rho}$.

Numerical experiments. In all numerical experiments performed, we observe a truly remarkable agreement with the theoretical predictions (see Figure 2 for a specific illustration). According to Eq.(18), by reducing the sector opening angle (i.e by increasing the values of the M), the resulting limit cycle radius $\mathcal{L}_{s,\rho}$ increases and the number of agents present in $V_{s,\rho}$ is reduced thus somehow invalidating the large population required for MF to be used. Even when $M = 50$, the couple of orbits realizations shown in Figure 3 show that analytical results, in particular Eq.(18), remain valid in this large M limit.

Generalization. By using the class of mixed-canonical dissipative dynamics [6] and following the same lines as those given in Proposition 1, we now can relax the cylindrical symmetry and write:

Proposition 2. *Consider the class of functions* $\mathcal{H}(x_1, x_2) : \mathbb{R}^2 \mapsto \mathbb{R}^+$ *for which the family of planar curves defined by* $[\mathcal{H}(x_1, x_2) - R] = 0$ *are closed* $\forall\ R > 0$ *and do not intersect for different values of* R*'s. Introduce the functional* $\mathcal{V}(\mathcal{H}) : \mathbb{R}^+ \mapsto \mathbb{R}$ *with* $\lim_{\mathcal{H}\to\infty} \mathcal{V}(\mathcal{H}) = \infty$. *Assume in addition that the values of the* $\mathcal{H}$*-derivatives* $\mathcal{V}'(0) < 0$ *and* $\mathcal{V}'(\mathcal{H}) \mid_{\mathcal{H}=C} = 0$ *and* C *is the unique value for which it holds. Then Eqs.*(1) *and* (9) *can be respectively generalized as:*

$$\begin{cases} d\mathbf{X}_k(t) = \mathbb{A}_k(\vec{\mathbf{X}})\, dt - \gamma \left\{\mathcal{V}'(\mathcal{H}(\mathbf{X}))\partial_{\mathbf{X}_k}\mathcal{H}(\mathbf{X}_k)\right\} dt + \sigma\, d\mathbf{W}_k(t), \qquad k = 1, 2, \cdots, N, \\ X_k(0) = X_{0,k}, \qquad \text{and} \qquad X_k(t) \in \mathbb{R}^2, \end{cases} \tag{19}$$

where

$$\mathbb{A}_k(\vec{\mathbf{X}}) = \begin{pmatrix} \frac{N_k(t)}{N} - \frac{1}{M} & \frac{N_k(t)}{N} \\ -\frac{N_k(t)}{N} & \frac{N_k(t)}{N} - \frac{1}{M} \end{pmatrix} \cdot \begin{pmatrix} \partial_{X_{1,k}}\mathcal{H}(\mathbf{X}_k) \\ \partial_{X_{2.k}}\mathcal{H}(\mathbf{X}_k) \end{pmatrix} \tag{20}$$

and

$$\begin{cases} dX_1(t) = \left[+\frac{1}{M}\partial_{X_2}\mathcal{H}(\mathbf{X}) - \gamma\left\{[\mathcal{V}'(\mathcal{H}(\mathbf{X})]\,\partial_{X_1}\mathcal{H}(\mathbf{X})\right\}\right] dt + \sigma dW_1(t), \\ dX_2(t) = \left[-\frac{1}{M}\partial_{X_1}\mathcal{H}(\mathbf{X}) - \gamma\left\{[\mathcal{V}'(\mathcal{H}(\mathbf{X})]\,\partial_{X_2}\mathcal{H}(\mathbf{X})\right\}\right] dt + \sigma dW_2(t). \end{cases} \tag{21}$$

The stationary measure Eq.(10) *here reads:*

$$P_s(\mathcal{H})\, d\mathcal{H} = \mathcal{Z}^{-1} \exp\left\{\frac{2\gamma}{\sigma^2}\,[\mathcal{V}(\mathcal{H})]\right\} d\mathcal{H}, \tag{22}$$

where $\mathcal{Z}$ *is the normalization constant.*

□

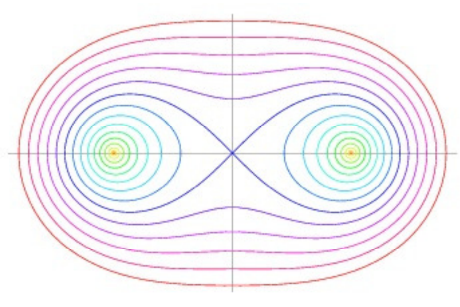

Figure 4: Typical shapes of the Cassini's ovals determined by the equation $\mathcal{H}(x_1, x_2) = \left[(x_1 - 1)^2 + x_2^2\right]\left[(x_1 + 1)^2 + x_2^2\right] = b^4$ for b-values ranging from $b = 0.1$ to 1.5.

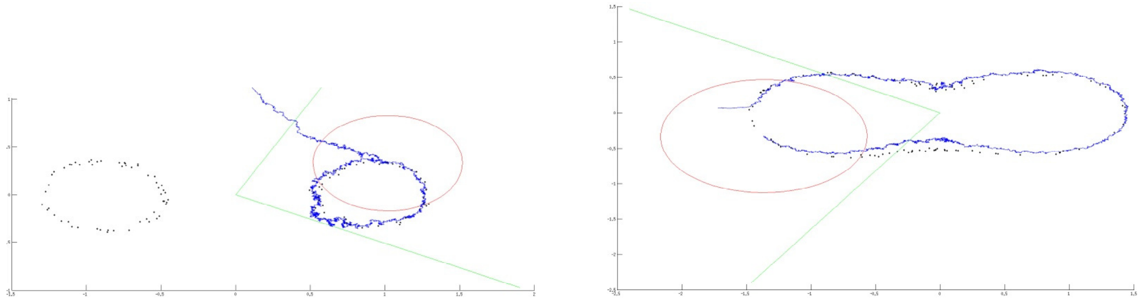

Figure 5: Left: Selection of a couple of limit cycling orbits obtained from the Cassini Hamiltonian Eq.(23) when the control parameters are set to $M = 4$ and $\rho = 0.4$.
Right: Single limit cycling trajectory for the Cassini Hamiltonian Eq.(23) but here with the control parameters set to $M = 4$ and $\rho = 0.8$.

Additional remarks.

a) Observe that Proposition 1 follows from the Proposition 2 in the rotationally symmetric case resulting when $\mathcal{H}(\mathbf{X}) = (1/2)\left[X_1^2 + X_2^2\right]$.

b) Contrary to Proposition 1, in Proposition 2 , neither the limit cycle nor the invariant measure $P_s(\mathcal{H})$ generally have a cylindrical symmetry. This precludes the possibility to analytically determine the selected consensus limit cycle (i.e we do not have in the general case a simple expression like the one given by Eq.(18)).

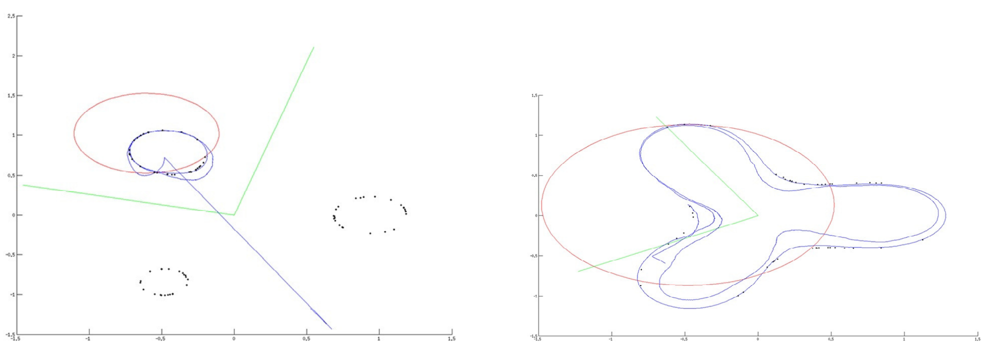

Figure 6: Left: Orbit generated by the $(\frac{2\pi}{3})$-symmetric Hamiltonian function: $\mathcal{H}(x_1, x_2) = \left[(x_1 - 1)^2 + (x_2)^2\right]\left[(x_1 + \frac{1}{2})^2 + (x_2 - \frac{\sqrt{3}}{2})^2\right]\left[(x_1 + \frac{1}{2})^2 + (x_2 + \frac{\sqrt{3}}{2})^2\right]$. Here we have $N = 100$ and the control parameters are set to $M = 4$ and $\rho = 0.5$.
Right: Here, all parameters are identical, except for the interaction range which is $\rho = 1$.

c) As an illustration of Proposition 2, we may consider the Cassini Hamiltonian function given by

$$\mathcal{H}(\mathbf{X}) = \left[(x_1 - 1)^2 + x_2^2\right]\left[(x_1 + 1)^2 + x_2^2\right] = b^4, \tag{23}$$

with the level orbits sketched in Figure 4. According to the values of M and ρ which ultimately will fix the size of the parameter b, we are in this case able to generate two different regimes. For large b a single closed consensus limit cycle is generated. Alternatively, for small b, the agents are shared into two clusters and evolve on two separated consensus limit cycles (see Figure 6.

d) Generalizing the previous Cassini ovals construction, one may construct Hamiltonian generating agents circulation on even more complex orbits. We provide an additional example in Figure 6.

3 Conclusions and perspectives

While agents with behavior-based interactions are relatively easy to implement, it is widely recognized that the underlying mathematical analysis of such models is generally difficult and often even impossible to perform completely. It is therefore quite remarkable that very simple analytical results can be derived for a whole class of dynamics which, due to its simplicity, offers potential for applications. Despite that for limited number of agents, typically one hundred in our present study, the mean-field approach can only be approximative, we nevertheless emphasize that all our numerical investigations still closely match the theoretical predictions. The resilience of our modeling approach opens several perspectives for implementations on actual agents. Several further research directions are naturally suggested by this contribution, among them:

a) *Extended MCD dynamics to higher dimensional spaces.* The role played here by the Hamiltonian function leading to a canonical motion on the plane can be extended. In particular one may consider, along the lines explained in [10], integrable canonical systems exhibiting additional constants of the motions. Using these extra constants of the motion, one will be able to stabilize the swarm motion along orbits in higher dimensions.

b) *Heterogeneity in agents and soft control of swarms.* Instead of focusing on homogeneous agents and by following the work [5], we intend to use the context of MCD to study the possibility to influence (i.e. *soft controlling*), the behavior by the introduction into the society of a single "fake" agent (i.e. a *shill*) playing the role of a *leader* which can be externally controlled.

c) *Resilience of the modeling.* In Eq.(2), we used the Euclidean norm to define $V_{k,\rho}(t)$, the instantaneous neighboring agents in Eq.(3). To match specific applications, other type of norms could be used to redefine the interactions.

Acknowledgment This research has been partly supported by the Swiss National Fund for Scientific research and the ESF project *"Exploring the Physics of Small Devices"*.

References

[1] F. Cucker and S. Smale. Emergent behavior in flocks. *IEEE Transactions on Automatic Control*, 52(5), 2007.

[2] T. D. Frank. *Nonlinear Fokker-Planck Equations.* Springer series in Synergetics. Springer: Complexity, 2005.

[3] V. Gazi and B. Fidan. *Coordination and control of multi-agent dynamic systems: Models and approaches*, volume 4433 LNCS of *Lecture Notes in Computer Science (including subseries Lecture Notes in Artificial Intelligence and Lecture Notes in Bioinformatics).* Springer, 2007.

[4] V. Gazi and K. M. Passino. A class of attractions/repulsion functions for stable swarm aggregations. *International Journal of Control*, 77(18):1567–1579, 2004.

[5] J. Han, M. Li, and L. Guo. Soft control on collective behavior of a group of autonomous agents by a shill agent. *Journal of Systems Science and Complexity*, 19(1):54–62, 2006.

[6] M.-O. Hongler and D. M. Ryter. Hard mode stationary states generated by fluctuations. *Zeitschrift für Physik B Condensed Matter and Quanta*, 31(3):333–337, 1978.

[7] M. A. Hsieh, V. Kumar, and L. Chaimowicz. Decentralized controllers for shape generation with robotic swarms. *Robotica*, 26(5):691–701, 2008.

[8] H. P. McKean Jr. A class of markov processes assocaietd with nonlinear parabolic equations. *Proc. Natl. Acad. Sci USA*, 56(6):1907–1911, 1966.

[9] Craig W. Reynolds. Flocks, herds, and schools: A distributed behavioral model. *Computers (ACM)*, 21(4):25–34, 1987. Cited By (since 1996): 1704.

[10] F. Schweitzer, W. Ebeling, and B. Tilch. Statistical mechanics of canonical-dissipative systems and applications to swarm dynamics. *Physical Review E - Statistical, Nonlinear, and Soft Matter Physics*, 64(2 I):211101–211112, 2001.

[11] R. Sepulchre, D. A. Paley, and N. E. Leonard. Stabilization of planar collective motion with limited communication. *IEEE Transactions on Automatic Control*, 53(3):706–719, 2008.

[12] T. Vicsek, A. Czirk, E. Ben-Jacob, I. Cohen, and O. Shochet. Novel type of phase transition in a system of self-driven particles. *Physical Review Letters*, 75(6):1226–1229, 1995. Cited By (since 1996): 1354.